Synthesis and behavior of responsive biobased polyurethane networks cross-linked by click chemistry

Khantutta-Kim Tremblay Parrado, Luc Avérous

Version of Record: https://www.sciencedirect.com/science/article/pii/S001430572031051X
Manuscript_6d60b20f2b90a8a29a04bce1abb66090

Synthesis and behavior of responsive biobased polyurethane networks cross-linked by click chemistry: Effect of the cross-linkers and backbone structures.

Khantutta-Kim Tremblay-Parrado[a] and Luc Avérous*[a]

[a] BioTeam/ICPEES-ECPM, UMR CNRS 7515, Université de Strasbourg, 25 rue Becquerel, 67087, Strasbourg, Cedex 2, France, luc.averous@unistra.fr

Distinct bismaleimides (BMIs) of differing molar masses and chemical architectures were studied as cross-linkers of different polyurethane (PUs) backbones containing pendant furan rings to form responsive biobased networks via the Diels-Alder (DA) reaction. The pendant furan rings were introduced during PU synthesis by the inclusion of a specific diol structure with furan groups and derived from oleic acid. The diol is denoted as the Furan Oligomer (FO) and its synthesis can respect green chemistry principles. The effects of varying the proportions of FO in cross-linked systems as well as the type of BMIs (aliphatic vs. aromatic) were particularly studied. The corresponding materials were fully analyzed through several complementary approaches to evaluate their physical, chemical and thermal properties and behaviors. PUs cross-linked by an aromatic BMI yield superior mechanical properties, whereas the chain length and structure clearly influenced the swelling, reprocessability and heat induced healing of the networks. The introduction of hard segments (HS) into the PU backbone was also examined in terms of micro-segregation. The effect of hydrogen bonding linked to HS in combination with the cross-links by DA would yield superior mechanical properties with good thermal recyclability and self-healing behaviors, to develop materials for advanced applications.

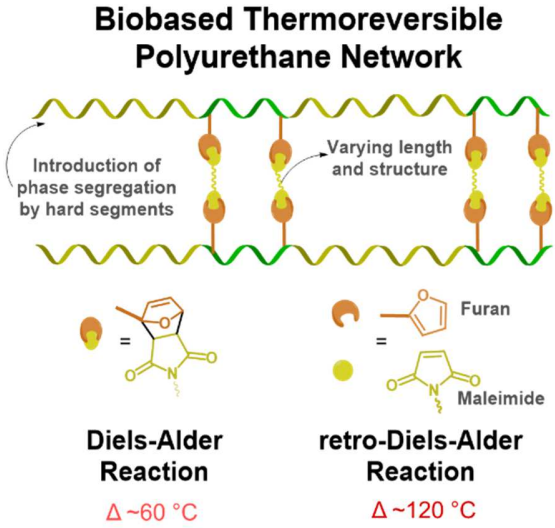

Introduction

The modern era was revolutionized by the invention and development of plastics, and as such plastics have gained prevalence in most aspects of our daily lives, with its existence found amongst consumer and industrial goods as well as medical devices. However, with its strong and constant production (mainly from fossil resources since the 1950s), plastics with its ubiquitous presence has hailed emerging concerns for its increasing appearance and dispersion in all environments throughout the planet (landfills, oceans, etc.) ensuing more and more lasting environmental impacts. Consequently, polymers and materials design should not only take in account the origin of materials (by developing for instance biobased and environmentally friendly materials) but as well as factor in advanced properties to manage the end of life as well as extending materials lifetimes. Cross-linked polymers (or thermosets) are a prominent type of material, consistently of up to 20% of the produced polymers) [1], mainly due to their high mechanical properties and chemical stability. Nevertheless, they have been mismanaged in their end of life, given their inability to be recycled by traditional techniques as that of thermoplastics.

One way to overcome these issues is by the incorporation of dynamic interactions into polymer networks to give rise to advanced properties such as self-healing and reprocessability, which in turn can extend the life time of materials and reduced energy and resource consumption to yield circular and sustainable material design approach [2]. Polymer networks with dynamic cross-links have recently skewed the conventional division between thermoplastics and thermosets. The recent work of Sumerlin et al. outlines the fundamental theory of these dynamic polymer networks and provides a critical assessment of their status [3]. Generally, these networks are based on dynamic covalent bonds which are assembled and disassembled by “associative” or “dissociative” processes by the exposure to external stimuli (often thermal) or autonomously [4]. Cross-linked polymers containing dynamic covalent bonds were coined by Kloxin et al. as Covalent Adaptive Networks (CANs) [5]. Associative CANs consists of bond exchange between polymer chains, with a preserved cross-linking density, as a new covalent bond can only be formed if another has been broken. As discovered by Liebler and co-workers, vitrimers are an example of this [6], and can also be exclusively biobased [7]. Alternatively, dissociative CANs exhibit chemical bond exchanges where bonds are first broken and reformed again. Many networks containing thermoreversible cross-linking covalent chemistries have been explored such as the Diels-Alder (DA) cycloaddition [8], hindered urea exchange [9], and 1,2,3-trazolium salts [10]. The thermoreversible furan-maleimide [4+2] cycloaddition DA reaction is the most prominently studied reversible chemistry used to synthesize dissociative CANs [11]. Regardless of the corresponding chemistry, the association between the design of these thermosets and the notion of recyclability at the end of life using dynamic cross-links allows us to develop sustainable materials.

Polyurethanes (PUs) are a versatile and major polymer family that can be tuned for a wide range of applications, for instance, the construction, automotive and medical industry. The tunability of PUs is notably possible by controlling the occurrence of micro-phase separation consisting of hard segments (HS) and soft segments (SS). The SS phase of PUs brings flexibility to the materials, whereas the HS (composed generally of a diisocyanate and chain extender) contributes to strength and rigidity by physical cross-links. Consequently, PUs are ranked 6th in terms of worldwide production [12]. Their chemical structures can also be tuned for the incorporation of thermoreversible chemistry such as that of the DA reaction to further enhance the sustainability of cross-linked PUs [13-15]. Nevertheless, to design sustainable materials, they must be derived from renewable resources. Nowadays, the biobased PU market is expanding with a particular emphasis on use of vegetable oils consisting of adequate macromolecular architectures for the developments of polyols for thermosets [16], or for thermoplastic PU applications [17, 18], by controlling several parameters such as the functionality.

In the last decade, there seems to be an increasing research in developing biobased CANs from diverse biobased resources such as lignins [19, 20], tannins [21], alginate [22, 23], chitosan [24], starch [25], 5-hydroxymethyfurfural [26], natural rubber [27], or vegetable oils [28]. Nevertheless, according to the literature, the development of dynamic biobased PU architectures is until now largely limited [29]. In a recent work [30], we have addressed this challenge by synthesizing reversibly cross-linked PUs based on vegetable oils using the thermally reversible furan-maleimide DA reaction. The DA reaction between furan and maleimide functions is defined as a click cycloaddition reaction and occurs at modest temperatures (below 90 °C), whereas the retro-DA (r-DA) reaction, occurs between 110 and 130 °C [8]. In this recent work [30], a cross-linked PU system was proven to be thermally recyclable and self-healable by the incorporation of a diol containing pendant furan rings called the Furan Oligomer (FO), which

was derived from oleic acid. The pendant furan rings of the PU backbone were reacted with a short poly(propylene oxide) (PPO) based bismaleimide (BMI) to form cross-linking points.

The aim of this study is to examine more particularly the effect the BMI structure and length (Scheme 1 – Route 1) onto the polymer properties such as the thermal recyclability and heat induced healing of the corresponding biobased PU networks. Furthermore, new macromolecular architectures with increased hydrogen bonding content were developed (Scheme 1– Route 2), by the incorporation of hard segments into the PU backbone via the addition of 1,4 – butanediol. All these different macromolecular architectures were synthesizing by prioritizing green chemistry principles (such limiting use of hazardous materials and solvents) and compared through different approaches.

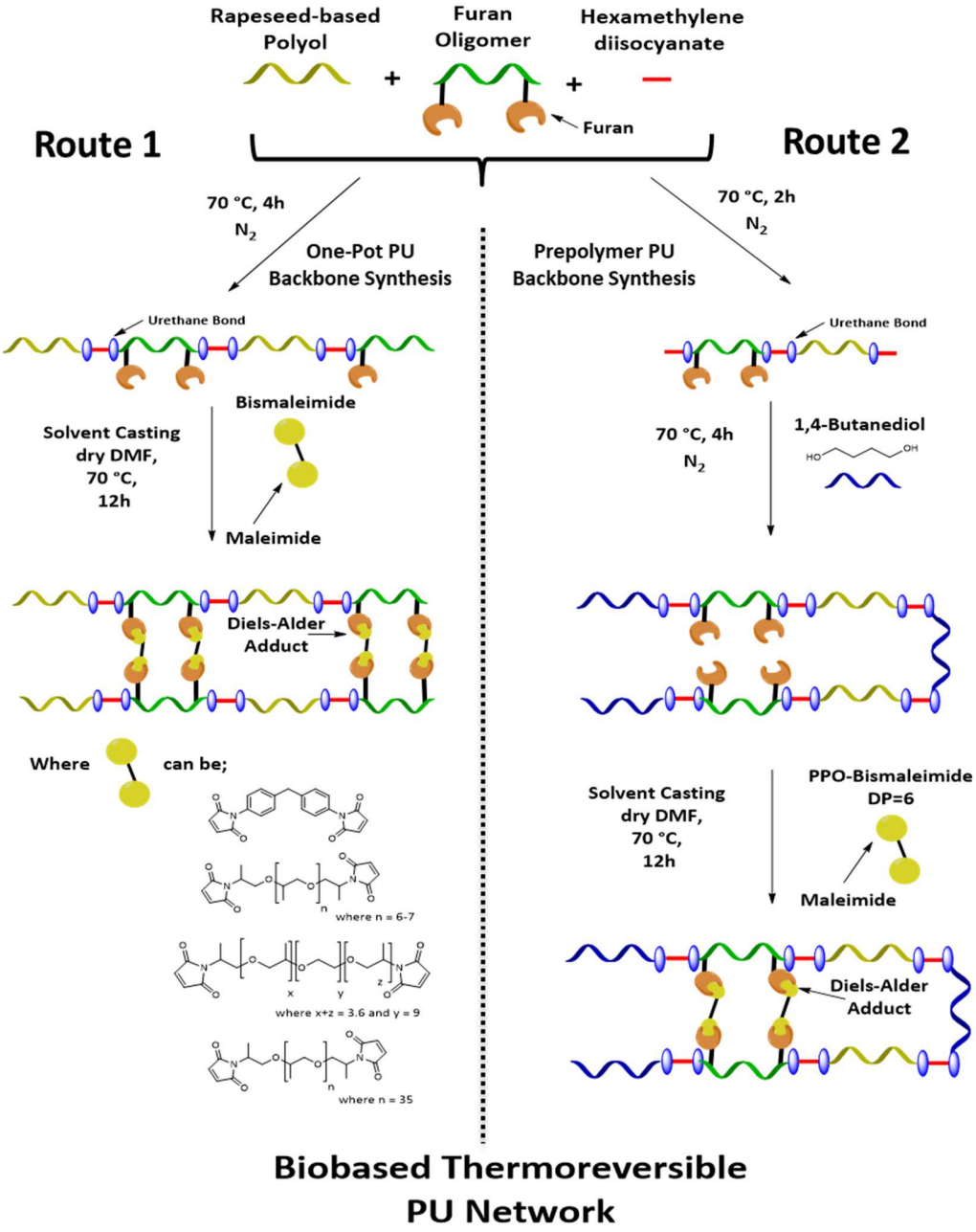

Scheme 1 – Illustration of the general synthesis of biobased thermoreversible PU-based systems using FO

Experimental Section

Reagents and materials

Octadec-9-enoic acid (OA) from sunflower oil was supplied by ITERG. Acid value is 185 mg KOH per g. Biobased polyester polyol (purchased from Oleon) was derived from dimeric fatty acids from rapeseed oil with purity greater than 98% and weight average molar mass (M_w) around 3 000 g/mol. Hydroxyl and acid values were 33.7 and 0.253 mg/g KOH, respectively. The cross-linkers are different bismaleimides (BMI) such as poly(propylene oxide) bismaleimide (degree of polymerization or DP = 6 and 33) and poly(propylene oxide)-b-poly(ethylene oxide)-b-poly(propylene oxide) bismaleimide were obtained from Specific Polymers (Castries, France). 4-dimethylaminopyridine (DMAP, 99%), 2-chloro-4,4,5,5-tetramethyl-1,3,2-dioxaphospholane (CL-TDP, 95%), Furan-2-ylmethanol (FM, 98%), hydrogen peroxide (H_2O_2, 30% *w/v* aqueous solution), chromium (III) acetylacetonate (99.99%), [D_6]dimethyl sulfoxide (DMSO, 100%, 99.96% atom D) and cholesterol (>99) were purchased from Sigma Aldrich. N,N'-dicyclohexylcarboiimide (DCC, 99%), chloroform-d ($CDCl_3$, 100%, 99.96% atom D), 1,1′-(Methylenedi-4,1-phenylene)bismaleimide (95%, MPBMI) and $HSbF_6$ (65% *w/w* aqueous solution), were purchased from Alfa Aesar. Dichloromethane dried over molecular sieve (DCM, >99%, stabilized with amylene) and diethyl ether (stabilized with BHT) were purchased from Carlo Erba. N,N-dimethylformamide (DMF, 99.8%) Glacial acetic acid (GAA, >99%) and 1,4- Butanediol (BDO, 98%) were purchased from Fisher Scientific. Amberlite IR-120 H, Toluene (100%), 2,3,4,5,6-pentafluorobenzaldehyde (PFB,98%) and hexamethylene diisocyanate (HDI, 99%) was purchased from Fluka Chemicals, VWR Chemicals, Fluorochem, and Acros Organics, respectively. Most of these reagents and solvents were used without additional purification.

Syntheses and material processing

Synthesis of Furan Oligomer from oleic acid

The Furan Oligomer (FO) was synthesized by a previously reported 3-step synthesis procedure [30]. The detailed procedure can be found in the Supporting Information (SI). First, the esterification of Octadec-9-enoic acid (OA) by furan-2-ylmethanol in mild conditions by a Steglich Esterification was achieved. *N,N'*-dicyclohexylcarboiimide (DCC) was used as an activating agent, whereas 4-dimethylaminopyridine (DMAP) was used as a catalyst. This was followed by the Prilezhaev reaction to accomplish the in-situ epoxidation of the sole alkene bond on the fatty aliphatic chain by the use of H_2O_2 and glacial acetic acid in toluene. Lastly, FO diol structure was attained by acid-catalyzed ring-opening polymerization (ROP) using fluoroantimonic acid, $HSbF_6$, and water to control and limit the polymerization.

Diels-Alder and retro-Diels-Alder reaction between FO and different BMIs

To explore the dynamicity of the DA reaction between the furan moieties of the FO and maleimide moieties of BMIs, FO and each BMI were mixed together with a furan / maleimide molar ratio of 1, in a small flask and then dissolved in DMSO and exposed to different heating cycles. After 24 h exposure to 60 °C without stirring gelation occurs due to the DA reaction. To prove the r-DA reaction, the flask was exposed to 120 °C for 1 h. The mixture returns to a disassembled state. Each heating step was repeated another time. Final gels were washed with water, dried and examined by FTIR to compare with spectra of the initial system.

Synthesis of PUs containing FO

Rapeseed polyester polyol, FO as well as glassware were previously dried. PUs films were synthesized using different amounts of FO under nitrogen flow. For the synthesis of PU containing 20% FO the formulation included 11.8 mmol of OH from rapeseed polyester polyol, 3.01 mmol OH from FO and 15.5 mmol NCO from HDI, stirred mechanically for 3-4 h. The –NCO/-OH ratio was established to 1.05 for all syntheses.

Synthesis of PUs based on FO and BDO (with HS)

All glassware and reactants were previously dried. A single type of PU containing FO and BDO was prepared with a -NCO/-OH ratio equal to 1.05: 1, with a hard segment (HS) content of 20 %. This type of PU was synthesized by a two-step prepolymer process. In a first step, the polyol (15.8 g, 9.52 mmol OH,) FO (1.75 g, 2.38 mmol OH) and HDI (3.27 g, 38.9 mmol NCO) was reacted for 2 h in a three-necked, round-bottom flask, under a nitrogen flow, mechanical stirring at 70 °C. During the synthesis a sample was extracted to determine the NCO content to control the NCO consumption during the reaction in order to determine the proper amount of BDO chain extender to be

added. It was calculated for this experiment that the NCO content for the prepolymer should approximately be 5.4%. This NCO content result was used to determine the precise amount of BDO (≈ 1.13 g of BDO) to be added. The BDO was added and let react for 3 h and followed by FTIR.

Cross-linking of PUs

After the initial synthesis of linear PU, dry DMF was added in decrease the viscosity of mixing. The respective BMI was added in the required amount (to yield an overall furan to maleimide moiety ratio 1:1 between FO and BMI). In order for the DA reaction and cross-linking to occur the contents were stirred overnight at 70 °C. Then, the solution was transferred into a polytetrafluoroethylene mold for solvent casting by slow evaporation of DMF for 48 h at 70 °C followed by 24 h at 70 °C under vacuum to remove traces of solvent.

Methods and characterization techniques

Iodine value (IV) was determined using the Wijs method to quantify the double bond content according to ISO 3961:2018(E)

A specific method has been performed to determine the amount of isocyanate that reacts with on equivalent of *N*-dibutylamine, and gives NCO content by weight percent. A sample of the prepolymer (≈ 1.2 g) was diluted in a standard solution (20 mL) of dibutylamine 0.2M in THF, for a reaction between the excess diisocyanate. The excess amine was back-titrated with a 0.5 aqueous solution of HCl. NCO content by weight percent was determined using Equation (1):

$$\%NCO = \frac{(V_{blank} - V_s) * 42 * 0.1}{m_s} \quad (1)$$

in which V_{blank} (mL) is the HCl solution volume required for a blank titration of the dibutylamine solution, while V_s is the volume required for the prepolymer titration and m_s is the prepolymer weight. It was calculated from this experiment that the NCO content for the prepolymer should approximately 5.4%. This result was used for the addition for the precise amount of BDO (≈ 1.13 g of BDO). The BDO was added and left reacting for 3 h and followed by FTIR.

All NMR spectra were recorded on a Bruker Ascend 400 or 500 MHz spectrometer. Sample were dissolved in deuterated chloroform ($CDCl_3$) or deuterated dimethyl sulfoxide ([D_6]DMSO) with contents between 8-10 and 20-30 mg/mL for ^{1}H-NMR and ^{13}C-NMR spectroscopy, respectively. The calibration of ^{1}H- and ^{13}C-NMR spectra was performed using the chloroform peaks at δ = 7.26 and 77.16 ppm, respectively and DMSO peak at δ = 2.50 ppm as references. ^{31}P NMR analysis was performed by 2-chloro-4,4,5,5-tetramethyl-1,3,2-dioxaphospholane as phosphytilating agent. Scans (128) were recorded with a 15 s delay and a spectral width of 80 ppm (180-100 ppm). Cholesterol was used as an internal standard, as described in standard protocols [34]. In the case of quantitative ^{1}H NMR spectroscopic analysis, 20 mg was dissolved in [D_6]DMSO (0.5 mL) for each sample before the addition of a standard solution (100 µL) of pentafluorobenzaldehyde in [D_6]DMSO. 32 scans were collected 10 s delay.

For FTIR spectroscopy of experimental samples, a blank background was performed prior to examining samples (32 scans, resolution 4 cm^{-1}) on a Nicolet 380 spectrometer equipped with an ATR diamond module (FTIR-ATR) in reflection mode.

Dynamic rheological measurements were performed with a TA Instruments Discovery HR-3, using plate-plate parallel geometry equipped with a Peltier temperature control system. The lower plate had a 60 mm diameter whereas the upper plate had a 25 mm diameter. Gel formation between FO and BMI studied by examining the progression of the (G´) and loss (G´´) modulus at 60 °C at a constant shear strain (1%), at 1 Hz. The gel point is defined at the gel time (t_{gel}) when the curves of G' and G'' crossover. The dynamicity of the gel formed on the viscometer was evaluated by exposing it heating cycles of 120 °C to disassemble the gel (r-DA reaction) followed by 60 °C to re-assemble it (DA reaction). This heating cycles were repeated.

Sample weighing between 1-3 mg were evaluated by TGA (TA Instrument Hi-Res TGA Q5000) at a heating rate of 10 °C min^{-1} from 25 to 700 °C, without oxidative atmosphere, under nitrogen flow rate atmosphere at 25 mL min^{-1}.

In standard aluminium pans, samples between 1 to 3 mg by weight were examined by DSC (TA Instrument Q200) under nitrogen flow at 50 mL min^{-1}. To study the dynamicity between furan and maleimide moieties by DSC, FO and PPOBMI-DP6 were mixed together in equimolar equivalents of the moieties and placed in an aluminium pan and exposed to a heating ramp of 2.5 °C min^{-1} from -80 to 165 °C. For cross-linked PUs, a single heating ramp of 10 °C min^{-1} over the same aforementioned temperature range. Non crosslinked materials were evaluated using a cyclical heating ramp.

Uniaxial tensile testing was performed on an Instron model 5567 H, USA at strain rate of 20 mm min^{-1} on dumbbell specimens of approximately 30 X 5 X 1 mm^3. For each synthesized or reprocessed PU, five dumbbell samples were tested.

The swelling ratio (SR) for each PU was determined between dried (m_i) and swollen samples (m_s) in DMF according to Equation 2:

$$SR = \frac{m_s - m_i}{m_i} * 100 \quad (2)$$

PU samples of approximately 10-20 mg were swollen in 15 mL of solvent over an entire day. Three repetitions were examined for each PU formulation. The insoluble fraction (IF) was determined by drying the swollen sample (m_f) according to Equation 3:

$$IF = \frac{m_f}{m_i} * 100 \quad (3)$$

Reprocessability study of synthesized PUs was preformed using a LabTech Scientific hot press. PUs we cut into small pieces and placed in the middle of tile mold (10 cm x 10 cm x 1 mm) at 150 °C. The material was softened by a 10 min preheating cycle, followed by venting cycles, a pressing cycle of 15 min with applied force of 16 MPa. Prior to punching the film into dumbbell traction samples, the film was cured at 60 °C for 48 h, followed by 24 h at room temperature.

To study the self-healing behavior, dumbbell-shaped samples where cut in half and put back in contact and exposed to 120 °C for 1 h, followed by a 24 h exposure to 60 °C. Prior to tensile test, the sample was left 24 h at ambient temperature.

Results and Discussion

Analysis of synthesis of FO

The FO was synthesized from the acid moiety and alkene site of oleic acid (OA) as per a previous procedure [30]. As previously described OA underwent a Steglich esterification at ambient temperature using furan-2-lymethanol (FM) to yield furan-2-ylmethyl oleate (FMO). This step can also be accomplished via chemo-enzymatic esterification to adhere more adequately to green chemistry principles [31]. FMO was subjected to an in-situ epoxidation with the use of H_2O_2, glacial acetic acid (GAA) and an acid catalyst to yield the oxidizing agent, peroxyacetic acid, in toluene to yield furan-2-ylmethlyl 8-(3-octyloxiran-2-yl)octonoate (FMOO). This is a common method used in industry for the epoxidation of fatty acids. Finally, the oligomer diol, FO (Scheme 2), was obtained by acid-catalyzed ring-opening polymerization of FMOO using fluoroantimonic acid ($HSbF_6$) (1.5 wt %) and H_2O (0.7 mol equiv.) was performed in bulk. FO was fully characterized by FTIR, ^{31}P NMR and ^{1}H NMR spectroscopy. The corresponding data, which clearly confirms the successful synthesis is available in Supporting Information (SI) (Figure S1). The furan content of the FO was calculated as 1.88 mmol furan/g as an average of the distinctive signals determined by quantitative ^{1}H NMR spectroscopic analysis, whereas the hydroxyl value was determined to 54.1 mg KOH/g by quantitative ^{31}P

NMR spectroscopic analysis. This value was in good accordance with the results of a previous study [30]. All the corresponding data are summarized in SI (Table S1).

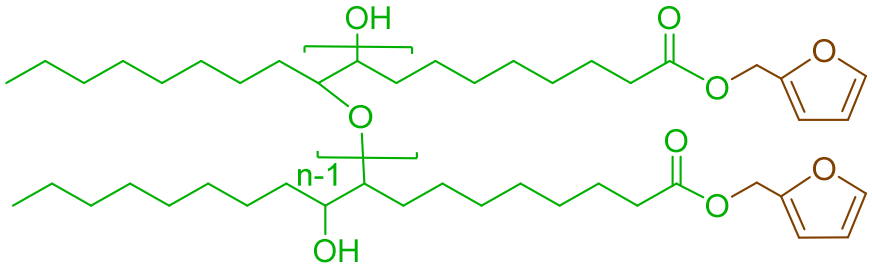

Scheme 2 – Chemical model structure of FO.

Analysis of DA and r-DA reactions between FO and different BMIs

In order to verify the occurrence of the DA reaction and consequently the r-DA, the FO was reacted with each BMI according to a previous procedure [30]. Four different aliphatic or aromatic bismaleimides were used with varied molar masses: 1,1′-(Methylenedi-4,1-phenylene) bismaleimide (MPBMI), PPO-based BMI with a degree of polymerization (DP) = 6 (PPOBMI-DP6), PPO-poly(ethylene-oxide)-based BMI with a DP = 13 (PPOPEOBMI-DP13) and PPO-based BMI with a DP = 33 (PPOBMI-DP33). The dynamicity (DA and r-DA) of the corresponding structures (FO with each BMI) was evaluated by dissolving FO and the respective BMI into DMSO under different heating processes at controlled temperatures and times. Figure 1-a shows the results of a system between FO and PPOBMI-DP6 dissolved in DMSO and exposed to heating cycles. As observed in Figure 1-a-i, the system is initially soluble is DMSO. Since the functionality in furan groups of FO is greater than two, a gel is then formed by DA reaction after an exposure to 60 °C for 24 h (Figure 1-a-ii). This step was followed by exposing the gel to 120 °C for 1 h. The gel is disassembled by r-DA reaction (Figure 1-a-iii). The heating cycle at 60 °C was repeated, and a gel network was reformed by DA reaction (Figure 1-a-iv). All other systems and results between FO and other BMIs can be found in SI (Figure S2). Similar observations can be made. To confirm the DA reaction took place, the system was evaluated before and after gel assembly by FTIR spectroscopy. The initial mix contained signals of free furan ($\tilde{\nu}$ = 739 and 1503 cm^{-1}) and maleimide rings ($\tilde{\nu}$ = 695 and 826 cm^{-1}) (Figure 1-b). Upon network assembly, the FTIR spectrum shows the loss of free furan and maleimide ring signals.

In order to follow the occurrence of thermal reaction between FO and PPOBMI-DP6, DSC was used. A stoichiometric system of FO and PPOBMI-DP6 was heated from -80 to 165 °C. Under the same conditions, FO and PPOBMI-DP6 were separately investigated. No thermodynamic phenomena occurred in the case of the separate reagents (Figure 1-c). In the thermogram of the mixed system (Figure 1-c, orange), an exothermic peak spans between 40 to 90°C, marking the DA reaction. This is followed by two endothermic peaks, corresponding to the r-DA. The peak of r-DA of the *endo* diastereomer occurred between 90 and 120 °C, meanwhile the r-DA of the *exo* diastereomer peak occurred by 120 and 145 °C [32]. This is highly indicative of the thermo-dynamicity of the cross-linking linkages with in PUs from FO and each of the four different BMIs.

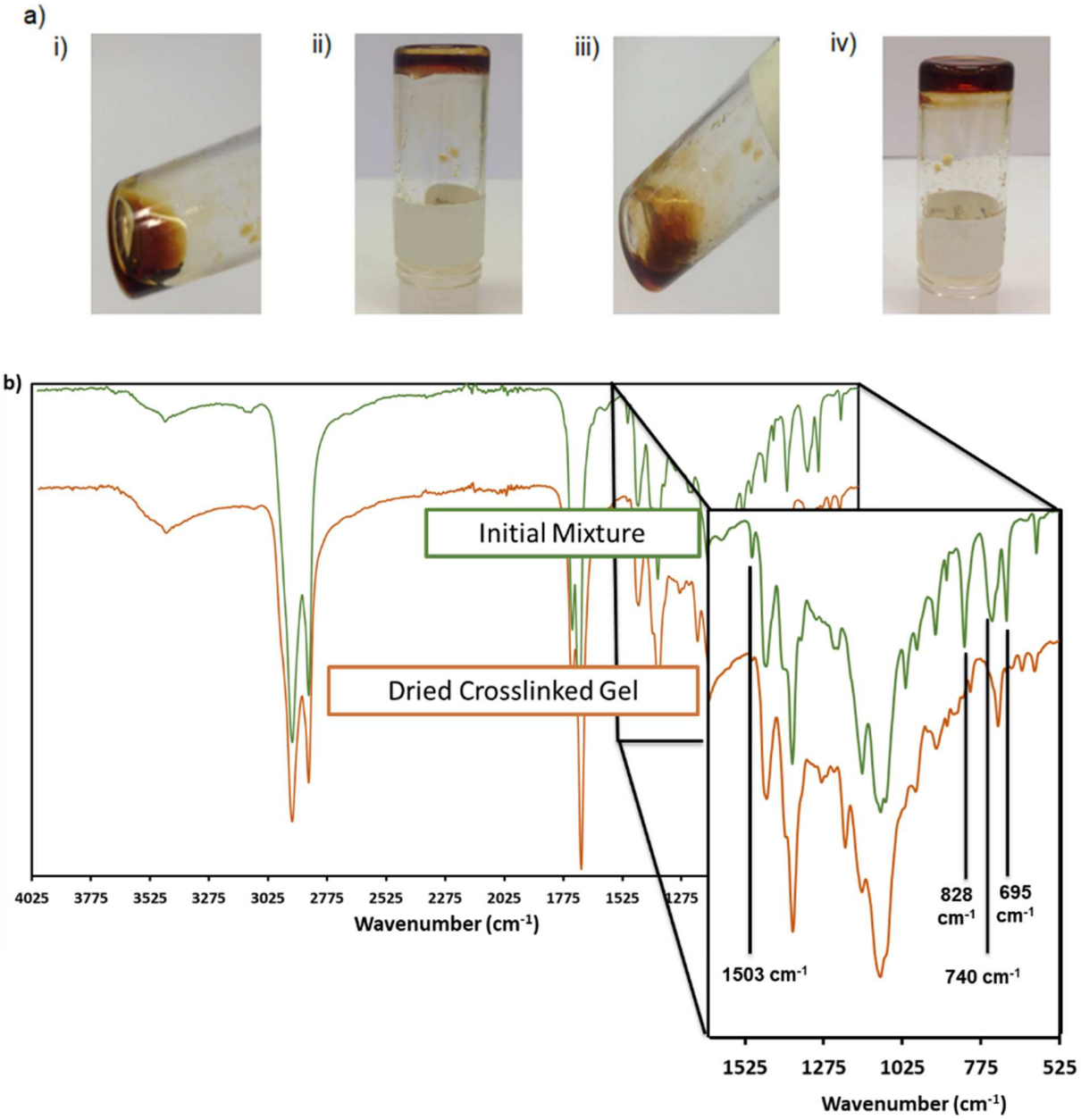

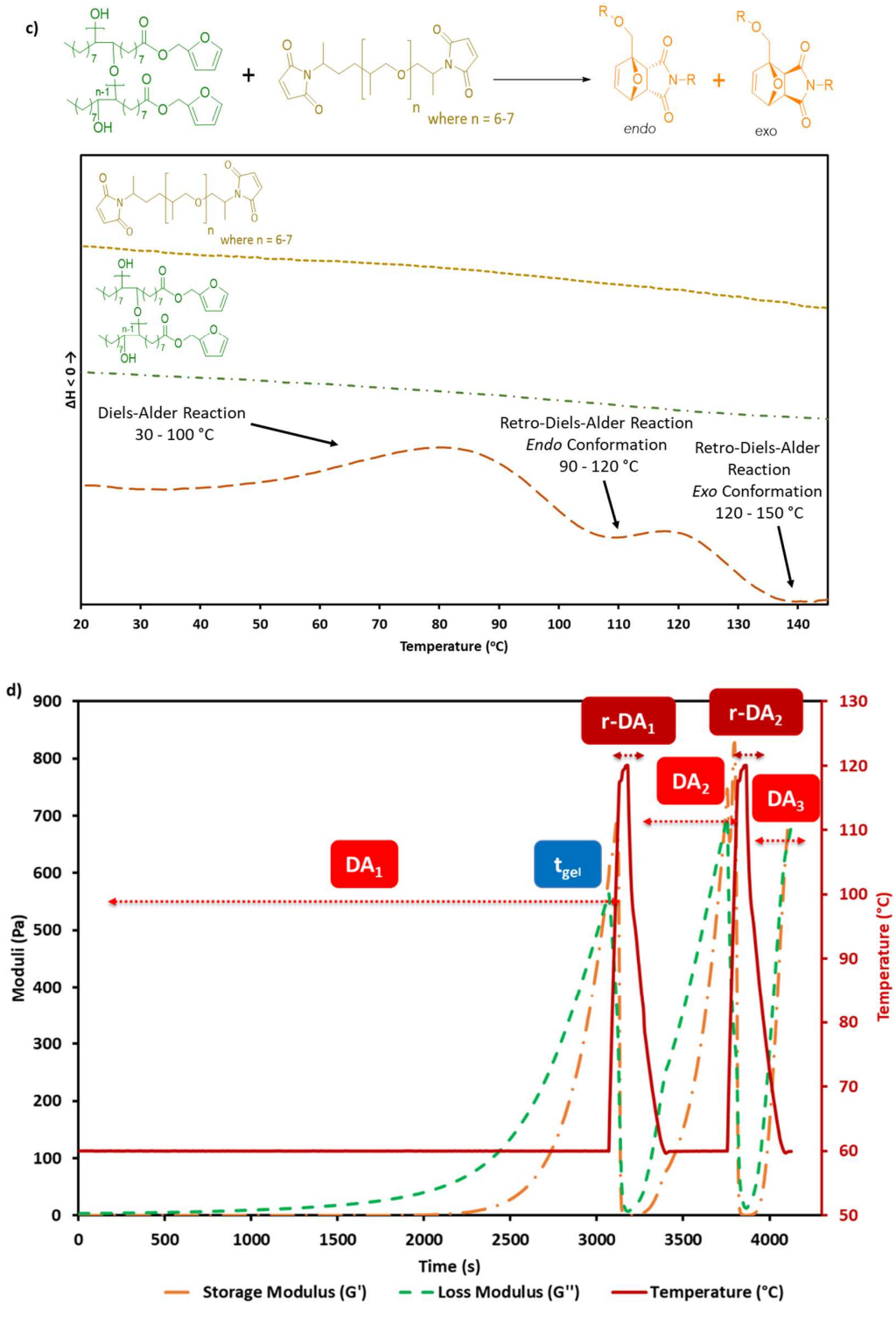

Figure 1 – (a) Photographs: (i) – Initial mixture of FO and PPOBMI-DP6; (ii) – mixture after 24 h at 60 °C, (iii) – mixture after additional 1 h at 120 °C; (iv) -mixture after additional 24 h at 60 °C; (b) FTIR spectra of initial mixture (green) and final dried cross-linked gel (orange). (c) DSC thermograms of PPOBMI-DP6, FO and the mixture of both, from 20 to 170 °C. (d) rheological behavior of gel formation between FO and PPOBMI-DP6.

To evaluate the rheological behavior of the gel formation between FO and liquid state BMIs, and to further study the DA reaction and r-DA between these reagents, dynamic experiments were performed. Gelation between FO and PPOBMI-DP6 occurred as the moduli overlap at 3046 s (51 min, G' ≈ G'' ≈ 538 Pa) (Figure 1-d). To study the reversibility of the gel, heating steps were induced; 60 °C for the DA and 120 °C for r-DA. Upon the 120 °C heating steps (r-DA), the gel disassembled and the moduli descended back to zero. The network was assembled two additional times with shorter gelation times. The same experiments were conducted between FO and different viscous state BMIs and can be found in SI (Figure S3) with the exception of MPBMI as it a powder that only melts at temperatures above 150 °C. Table 1 summarizes these experiments. It was observed that as the length of the BMI increased, the longer the time interval required to achieve initial gelation times (3046 and 7401 s for PPOBMI-DP6 and PPOBMI-DP33, respectively) and the weaker these gels appeared (538 and 185 Pa for PPOBMI-DP6 and PPOBMI-DP33, respectively).

Table 1 Summary of rheological behavior of gel formation between FO and BMIs.

Gel type	Time to gel point [s]	Moduli at gel point [Pa]
FO-PPOBMI-DP6	3046	538
FO-PPOPEOBMI-DP13	3209	294
FO-PPOBMI-DP33	7401	185

Elaboration and chemical structures of the biobased cross-linked PUs.

FO and different BMIs were used to obtain biobased PUs consisting of thermally dynamic DA adducts as cross-linking points. Via route 1 (Scheme 1), the portion of FO in the PU network was varied to prepare distinctive types of PUs. The FO content was varied from 10 to 30% of the total number of hydroxyl moles required to prepare PUs with a final NCO/OH ratio of 1.05. Given the low hydroxyl values of the polyol and FO, the required mass of these reagents to synthesize PUs with such a NCO/OH ratio is high compared to the diisocyanate required. Allowing for minimal use of the hazardous diisocyanate, all the while yielding interesting and innovative molecular architectures. In order for cross-linking to take place, once the PU backbone was achieved, it was dissolved in small volume of dry DMF, followed by adding the appropriate amount of BMI and letting the solution stir overnight at 70 °C. In order to allow homogenous cross-linking to take place but as well prioritize green chemistry principles, cross-linking took place in minimal amounts of dry DMF to reduce the mixing viscosity. These solutions then underwent solvent casting in a PTFE square mold for 48 h at 70 °C followed by 24 h under vacuum at 70 °C. Three different PUs cross-linked by MPBMI were synthesized and denoted PU-FO10-MPBMI, PU-FO20-MPBMI or PU-FO30-MPBMI according to FO composition, 10, 20 or 30% of the total hydroxyl moles required, respectively. To evaluate the influence of the BMI chemical structure and length (molar mass) on the behavior of the resulting cross-linked biobased PUs (mechanical, reprocessing and healing properties), PUs with 20 % FO content were cross-linked with three different BMIs, PPOBMI-DP6, PPOPEOBMI-DP13 or PPOBMI-DP33 (denoted as PU-FO20-PPOBMI-DP6, PU-FO20-PPOPEOBMI-DP13 or PU-FO20-PPOBMI-DP33), respectively. Two additional PUs were synthesized via route 2 (Scheme 1) to evaluate the impact of induced phase separation material properties. First a prepolymer was achieved using the rapeseed-based polyol, FO and HDI. FO was incorporated in order to represent 20% of the number of moles of hydroxyl required for the synthesis of the prepolymer. Once the prepolymer synthesis was achieved (followed by NCO content titration), BDO was added to yield a final PU with 20% of HS. The reference PU for this route was denoted as PU-HS20-FO20. In order to achieve a cross-linked system via the pendant furan rings of the FO in the soft segments of the PU, the reference PU was immediately dissolved in dry DMF, followed by the addition of appropriate amounts of PPOBMI-DP6. The solution was stirred overnight at 70 °C, in order for the DA reaction to take place. This final PU system was denoted PU-HS20-FO20-PPOBMI-DP6. Similarly, these solutions

underwent solvent casting in PTFE square molds to produce solid samples. Table 2 summarizes the different nomenclatures and the detailed formulations of all PU prepared systems.

Table 2 – Linear PU (reference) and cross-linked systems: nomenclature and corresponding formulations.

PU system	Type of system	FO content[a] [%]	Rapeseed polyol content [%]	Targeted HS content [%]	BMI[b] [equiv.]
PU-FO10-MPBMI	cross-link	10	90	0	1
PU-FO20-MPBMI	cross-link	20	80	0	1
PU-FO30-MPBMI	cross-link	30	70	0	1
PU-FO20-PPOBMI-DP6	cross-link	20	80	0	1
PU-FO20-PPOPEOBMI-DP13	cross-link	20	80	0	1
PU-FO20-PPOBMI-DP33	cross-link	20	80	0	1
PU-HS20-FO20	Linear (reference)	20	80	20	1
PU-HS20-FO20-PPOBMI-DP6	cross-link	20	80	20	1

[a] The FO content in the PU systems was varied from 0 to 30% of the total hydroxyl moles required to synthesize PUs with a final NCO/OH equivalent of 1.05. For samples PU-HS20-FO20 and PU-HS20-FO20-PPOBMI-DP6. [b] Equivalents of maleimide moiety from BMI with respect to furan moiety of FO.

In order to evaluate the achievement of the synthesis of all PU systems, they were evaluated by FTIR spectroscopy. Furthermore, even PU-HS20-FO20-DP6, a reference linear PU was insoluble in most common solvents ($CHCl_3$, DMSO, THF, DMF) and could not be evaluated by NMR spectroscopy. Figure 2 compares the FTIR spectra of FO, biobased polyol, BDO, PU-HS20-FO20, PU-HS20-FO20-PPOBMI-DP6 and PPOBMI-DP6. FTIR spectrum PU-HS20-FO20 (Figure -d), the signals at $\tilde{\nu}$ = 3375 and 1555 cm^{-1} linked with the -N-H stretching and bending appropriately of urethane group appear; the ester urethane stretch presents itself at $\tilde{\nu}$ = 1690 cm^{-1}. The hydroxyl signals (at $\tilde{\nu} \approx$ 3440 cm^{-1}) corresponding to the FO, rapeseed polyol and BDO disappeared due to the –NCO/-OH polyaddition. Figure -e displays the FTIR spectrum of PU-HS20-FO20-PPOBMI-DP6 which is quite similar to the spectrum of PU-HS20-FO20. Nevertheless, the presence of the carbonyls of the maleimides at $\tilde{\nu}$ = 1710 cm^{-1} from the addition of PPOBMI-DP6 becomes slightly apparent. Furthermore, because the PU-HS20-FO20-PPOBMI-DP6 is cross-linked by the DA reaction and a loss of free furan maleimide ring is observed. The FTIR spectra of cross-linked PUs without HS can be found in SI (Figure S4, Figure S5, Figure S6 and Figure S7).

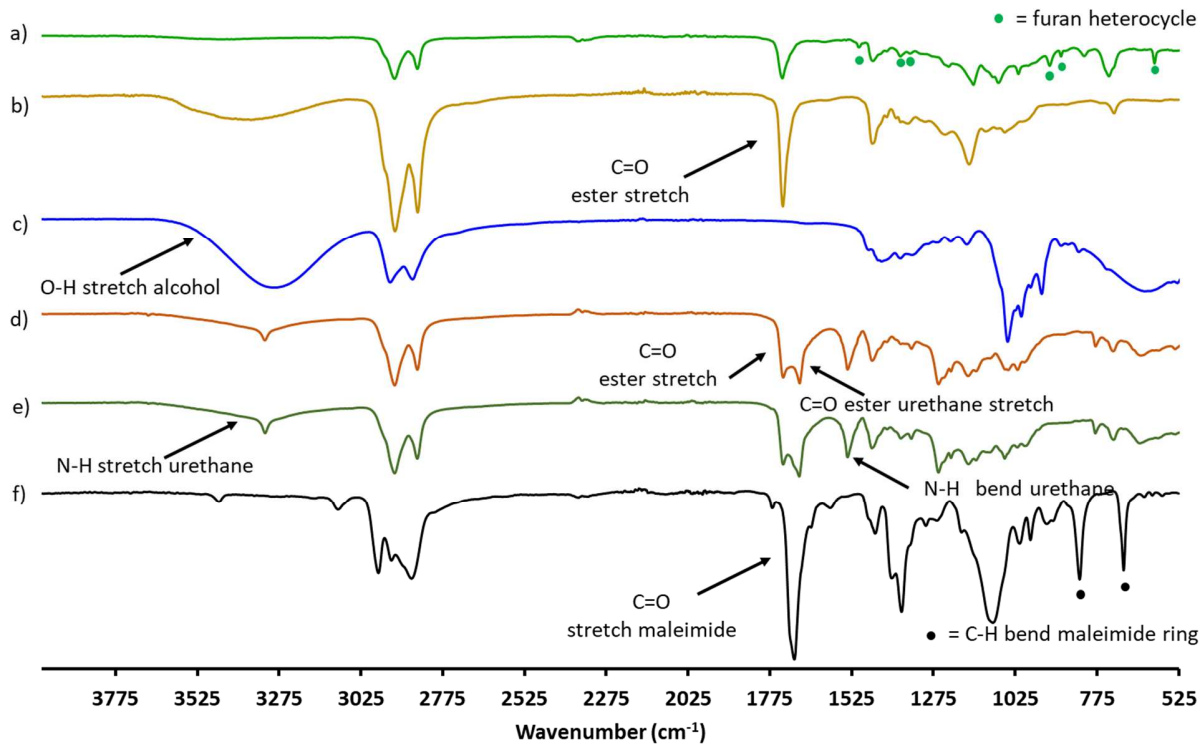

Figure 2 – FTIR spectra of (a) FO, (b) rapeseed polyol, (c) BDO, (d) PU-HS20-FO20, (e) PU-HS20-FO20-PPOBMI-DP6, and (f) PPOBMI-DP6.

Thermal behaviors of the cross-linked PUs

TGA was used to evaluate the thermal stability of the cross-linked PU materials. Table 3, displays the material properties and it can be observed that the initial thermal degradations ($T_{5\%}$) for the prepared PUs commence at temperatures greater than 150 °C. This suggests that a reprocessing at temperature of 150 °C based on r-DA can occur without thermal degradation. Similarly to previously reported results [30], an increase in FO content, decreases the $T_{5\%}$ in the PU networks. This is notable by the $T_{5\%}$ of PU-FO10-MPBMI compared to PU-FO30-MPBMI. Furthermore, all PU materials synthesized with a consistent amount of FO (20 %) and cross-linked by the different maleimides, remained with a $T_{5\%}$ steadily till around 330 °C. It is known that degradation of PUs is a complex multistep process, nevertheless, it generally accepted that an increase in HS also renders those materials more susceptible to thermal degradation, suggesting that initial degradation takes place predominantly in HS [33]. This is consistent with the results of PU-HS20-FO20 and PU-HS20-FO20-PPOBMI-DP6 which observed decreased and similar $T_{5\%}$ in comparison to all other PU networks. The thorough TGA results are found in SI (Figure S8).

Table 3 – Main results of the characterizations of cross-linked biobased PUs.

PU system	TGA $T_{5\%}$ [°C]	DSC T_g [°C]	Young's modulus [MPa]	σ[a] [MPa]	ε[b] [%]	SR[c] in DMF [%]	IF[d] [%]
PU-FO10-MPBMI	344	-51	1.86 ± 0.12	0.95 ± 0.08	265 ± 27	36.8 ± 1.0	97.5 ± 0.2
PU-FO20-MPBMI	332	-51	2.40 ± 0.22	1.10 ± 0.04	120 ± 5	45.6 ± 2.8	97.3 ± 0.4
PU-FO30-MPBMI	314	-51	2.22 ± 0.19	1.58 ± 0.16	118 ± 10	49.9 ± 1.5	96.4 ± 0.2
PU-FO20-PPOBMI-DP6	333	-50	1.65 ± 0.15	1.10 ± 0.03	129 ± 8	49.5 ± 2.6	96.7 ± 0.2
PU-FO20-PPOPEOBMI-DP13	324	-52	1.57 ± 0.21	0.86 ± 0.01	131 ± 5	54.5 ± 1.0	96.7 ± 0.3
PU-FO20-PPOBMI-DP33	326	-52	1.22 ± 0.10	0.80 ± 0.07	120 ± 7	71.5 ± 1.6	96.0 ± 0.2
PU-HS20-FO20	298	-50	11.84 ± 1.16	1.15 ± 0.11	30 ± 9	50.1 ± 1.7	95.6 ± 0.3
PU-HS20-FO20-PPOBMI-DP6	299	-49	14.47 ± 3.50	1.74 ± 0.20	24 ± 10	52.1 ± 2.5	96.1 ± 0.8

[a] Ultimate tensile strength. [b] Elongation at rupture. [c] SR=swelling ratio. [d] IF=insoluble fraction.

TGA results show that no degradation occurs in the studied DSC temperature range. Main DSC results are summarized in Table 3. Detailed DSC thermograms are found in SI (Figure S9). The T_g for all materials remain close to -51 °C. In a previous study [30], it was observed that networks containing increasing amounts of FO, (and increased cross-linking density) displayed more pronounced endothermic r-DA peak between 90 and 150 °C. This was also observed in series of PUs cross-linked by MPBMI (PU-FO10-MPBBMI, PU-FO20-MPBMI and PU-FO30-MPBMI) as shown in SI (Figure S10-a). Furthermore, for the series of PUs cross-linked with varied BMIs and consistent amount of FO (20 %), as for the increased length of the BMI, a decrease is observed in the prominence of the endothermic related to the r-DA reaction (Figure 2-a). The increase in the length of the BMIs decreased the cross-linking density by weight of the materials. A slight decrease in the T_g of PU-HS20-FO20-PPOBMI-DP6 was observed, when compared to its linear counterpart. Furthermore, as observed in Figure 2-b, the thermograms of cross-linked PU-HS20-FO20-PPOBMI-DP6 displayed the appearance of an endothermic signal between 90 and 150 °C correlating to the r-DA reaction. Contrastingly, without BMI, the reference PU counterpart remained unchanged.

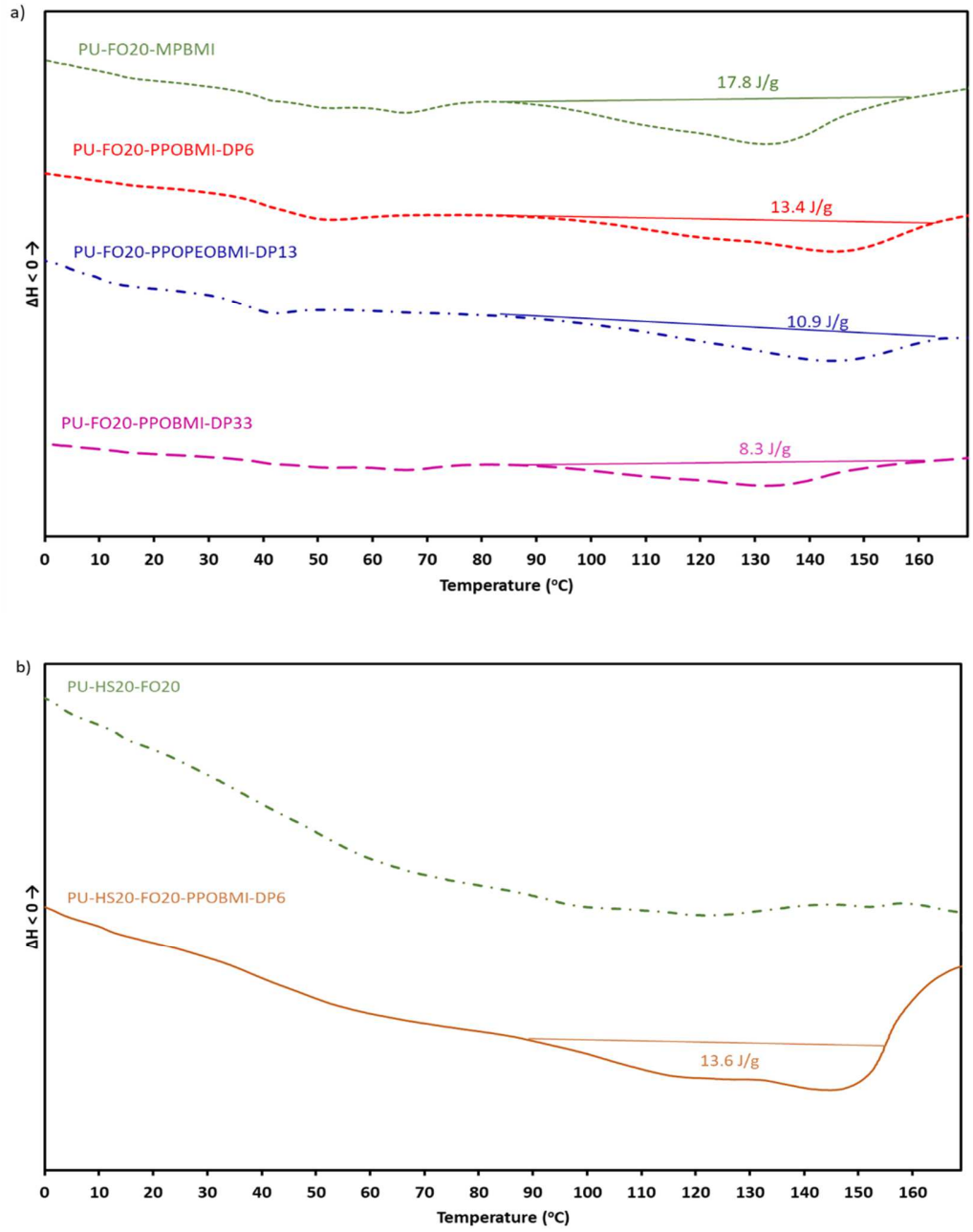

Figure 2 – Thermograms of (a) PU-FO20-MPBMI, PU-FO20-PPOBMI-DP6, PU-FO20-PPOPEOBMI-DP13, PU-FO20-PPOBMI-DP33 and (b) PU-HS20-FO20, PU-HS20-FO20-PPOBMI-DP6 from 0 to 170 °C.

Mechanical and swelling behaviors of the cross-linked PUs

All PUs synthesized were evaluated for their mechanical properties by uniaxial tensile testing at room temperature to analyze the influence of the structure and length of the BMIs. Main results were summarized in Table 3. The PUs series cross-linked by MPBMI with increasing amount of FO displayed a similar trend as cross-linked PUs in a previous study [30], by a PPO-based BMI with a DP = 3. That is, with increasing amount of FO (and consequently increasing cross-linking density), PUs materials displayed behaviors from thermoplastic elastomer (PU-FO10-MPBMI) to thermoset (PU-FO30-MPBMI) with an increase of tensile strength and a decrease of maximum elongation (Figure 3-a). Furthermore, in comparison to previous published results [30], the Young's modulus and

tensile strength of this PU series considerably increased. This evolution are largely due to the rigid aromatic structure of MPBMI.

The material properties of PU series with FO (20 %) cross-linked by different BMIs (PU-FO20-MPBMI, PU-FO20-PPOBMI-DP6, PU-FO20-PPOPEOBMI-DP13 and PU-FO20-PPOBMI-DP33) yield interesting results. As seen in Figure 3-b, PU-FO20-MPBMI presents the highest Young's modulus and tensile strength, which are mainly due to the phenyl structure of the MPBMI. With linear aliphatic BMIs, the cross-linked materials yield relatively similar Young's modulus, tensile strength and elongation, regardless of their varying lengths and molar masses. Nevertheless, PU-FO20-PPOBMI-DP6 claims the highest average Young's modulus and tensile strength, and PU-FO20-PPOBMI-DP33 the lowest. Thus a slight decrease in the Young's modulus and tensile strength is observed when increasing the length of aliphatic BMI cross-linker used. Furthermore, entanglements have a higher prevalence of occurring for BMIs with the longest lengths and can be a contributing factor to explain the similar results achieved between these PU systems. Lastly, PUs containing HS, PU-HS20-FO20 and its cross-linked counterparts PU-HS20-FO20-PPOBMI-DP6, exhibit superior mechanical properties, as evidenced by the mechanical properties of the reference PU. As seen in Figure 3-c, the cross-linked counterpart, PU-HS20-FO20-PPOBMI-DP6, exhibited an increased Young's modulus, tensile strength and decrease elongation due to the presence of cross-linking points.

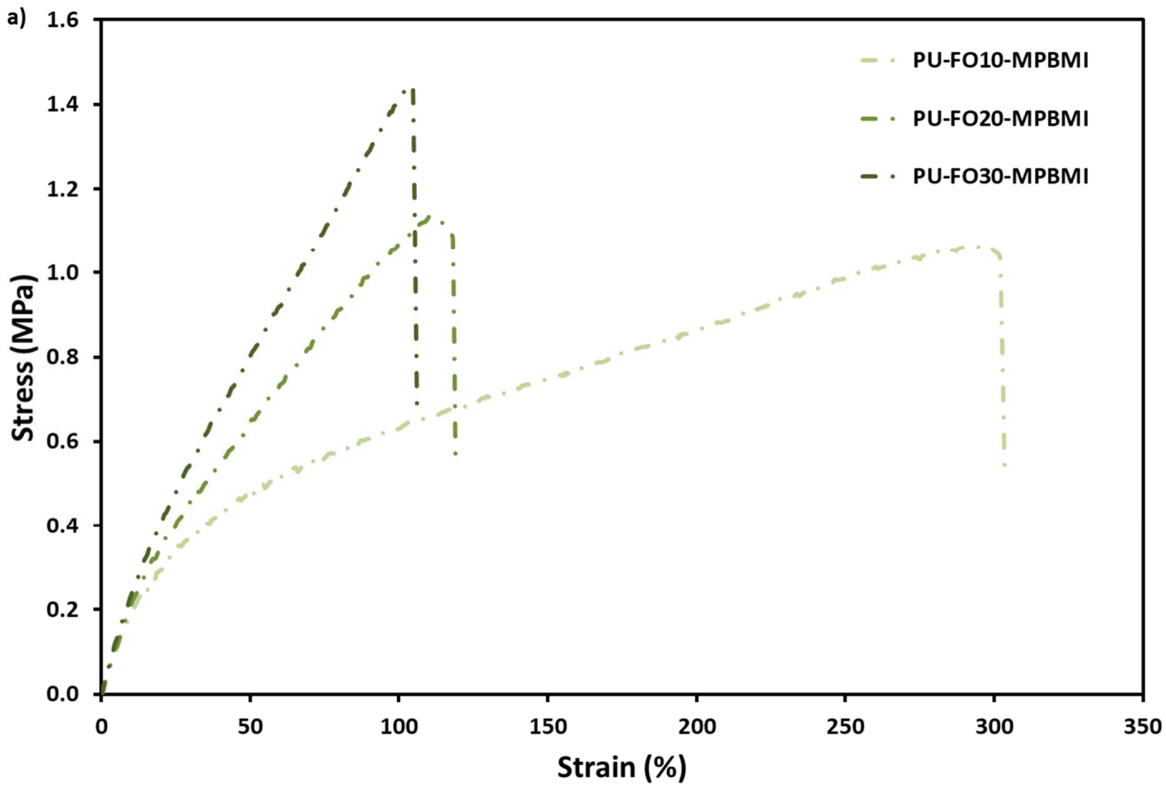

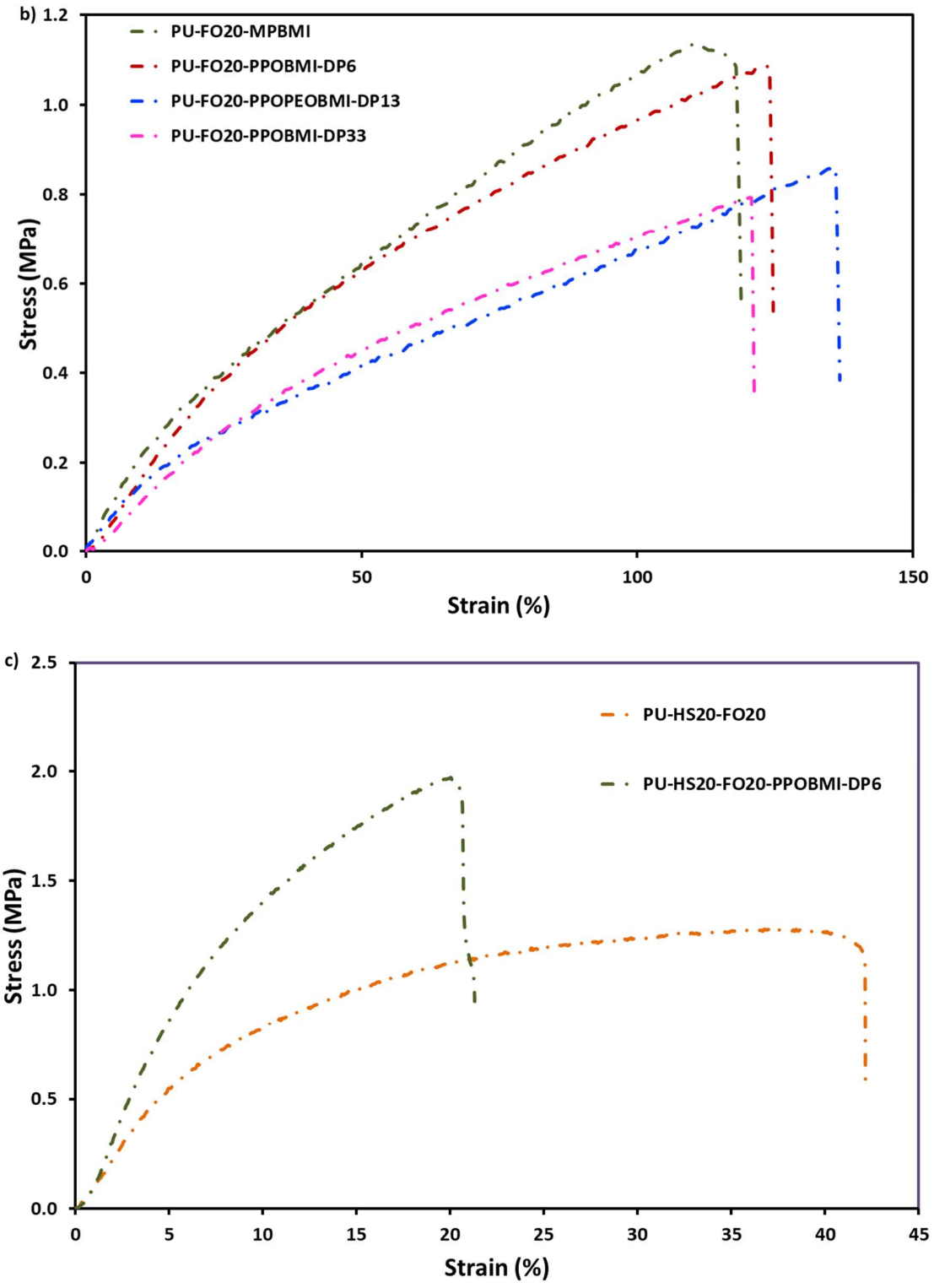

Figure 3 – Stress-strain curves of (a) PU-FO10-MPBMI, PU-FO20-MPBMI, PU-FO30-MPBMI (b) PU-FO20-PPOBMI-DP6, PU-FO20-PPOPEOBMI-DP13, PU-FO20-PPOBMI-DP33 and (c) PU-HS20-FO20, PU-HS20-FO20-PPOBMI-DP6.

The structures of the PU materials were also evaluated by swelling tests in DMF and the results are displayed in Table 3. As similarly observed in a previous study, although PU-FO10-MPBMI, PU-FO20-MPBMI, and PU-FO30-MPBMI, consist of increasing cross-linking densities, it was observed that the PU networks experienced higher swelling ratios (SRs), due to the affinity of the FO to swell in the given solvent. Furthermore, PU networks cross-linked with the aromatic BMI reveal to have the lowest SRs for PUs with respect to constant FO content, in part because MPBMI has the shortest length between maleimide groups. In the series of PUs prepared with equivalent amounts of FO (20%), cross-linked with increasing lengths of the aliphatic bismaleimides; it was observed that SRs increased with the BMI length. Finally, PUs containing HS, reference or cross-linked samples seemed to display statistically indifferentiable SRs despite the differences they yield in mechanical properties. It seems hydrogen bonding keeps the materials tightly packed when swelled and cross-linking in these proportions does not bring an evident effect in terms of swelling but it is evidenced in the evaluation of mechanical properties. All prepared materials were relatively insoluble with lowest insoluble fraction (IF) reported at 95.6 % for e.g., the linear reference PU-HS20-FO20.

Remendable and self-healing behaviors

Previous published results suggest that these PU materials could exhibit reprocessable and heat-induced self-healing behaviors [30]. Characterizing the reprocessability of all PUs synthesized was evaluated by comparing T_g and mechanical properties of the materials processed once by solvent casting, to that of PUs reprocessed by compression molding cycles as detailed in the Experimental section. The results of the mechanical properties of initial and reprocessed materials as well as a single sample of each initial material exposed to 120 °C treatment are shown Figure 4 (PUs without HS) and Figure 5 (PUs with HS). All detailed mechanical properties and T_g results are summarized in SI (Table S2). As seen in the SI, the T_g of reprocessed material did not vary substantially around that original materials of -51 °C likely attribute the T_g of SS of PU architectures. More extensive modulated DSC analyses could be used as means to explore the changes of the T_g of HS of these materials. These analyses could be also associated with DMTA characterizations to determine the changes of relaxation temperatures, which could be associated to T_g.

The reprocessability of the PU series containing varying FO contents and cross-linked by MPBMI were generally reprocessable over one reprocessing cycle for all materials (PU-FO10-MPBMI, PU-FO20-MPBMI and PU-FO30-MPBMI). However, PU-FO10-MPBMI and PU-FO20-MPBMI experienced a notable loss in the Young's modulus after a second reprocessing cycles, whereas PU-FO30-MPBMI evidenced diminished mechanical properties after a second reprocessing cycle on all fronts. In a previous study [30], a PU material was synthesized with 30 % substitution of FO and cross-linked with a PPO BMI DP = 3 would yield a confirmed reprocessable material after two compression molding reprocessing cycles. Thus, it can be concluded that although the aromatic nature for the MPBMI can yield superior mechanical properties, it can affect the reprocessing ability of the material with this particular procedure. A contributing factor effecting the reprocessing ability is the reduced local mobility of MPBMI in the material.

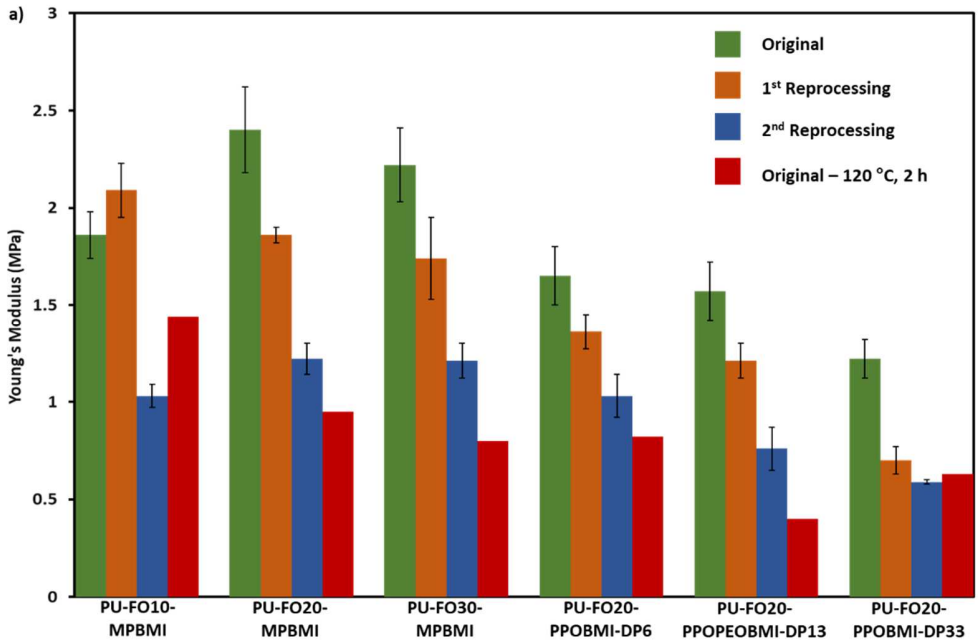

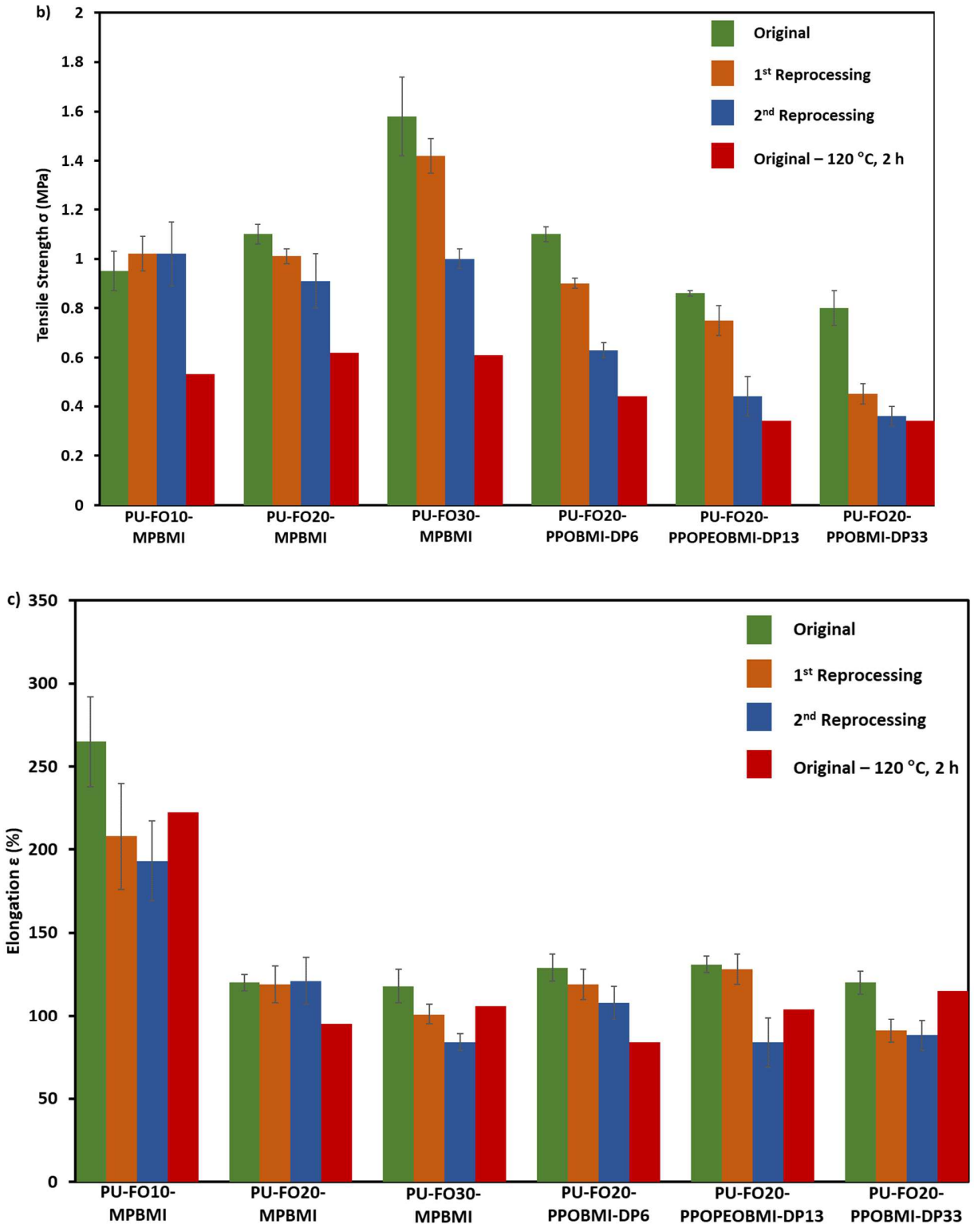

Figure 4 – Comparison of mechanical properties of biobased PUs: original, reprocessed and original heated to 120 °C, (a) Young's modulus, (b) tensile strength (σ), and (c) elongation (ε).

The effect of varying the BMI length and structure while keeping the FO content constant (20 %) was seen most prevalent in the ability of PU materials to be reprocessable by the corresponding reprocessing procedure. PU materials PU-FO20-MPBMI, PU-FO20-PPOBMI-DP6 and PU-FO20-PPOPEO-DP6 were generally reprocessable after one reprocessing cycles, with slight losses in Young's modulus. In contrast, PU-FO20-PPOBMI-DP33 experienced considerably diminished mechanical properties after a single reprocessing single. Upon a second reprocessing, PU materials PU-FO20-MPBMI, PU-FO20-PPOBMI-DP6 and PU-FO20-PPOPEO-DP6 experienced significant loss in mechanical properties, but slightly superior results when compared to a single original sample exposed to a 120 °C thermal treatment. For each type of PU material, a single dumbbell sample was exposed to a 120 °C thermal treatment and evaluated by uniaxial tensile test to evaluate a sample that mimics a material with relatively no cross-linking. It is indicative that upon a second reprocessing remnant cross-linking is apparent when compared to an original sample exposed to a 120 °C thermal treatment. Nevertheless, these results contrast with initially reported findings for similar PU systems cross-linked by a shorter PPO BMI DP = 3 and which were deemed reprocessable. Thus, increasing significantly the length of the BMIs can affect the reprocessing ability, by this reprocessing procedure. Dissociative CANs often exhibit different crosslink densities after reprocessing and thus effect mechanical properties for a multitude of reasons, such as: chain rearrangement, vitrification or cross-link degradation [5]. Furthermore, it is not to say that the PUs system cross-linked with longer chain BMIs could not exhibit enhanced reprocessing ability by a more adapted reprocessing procedure. As explained by Sumerlin and coworkers, two attributes profoundly impact the temperature-dependent viscoelastic behavior of dissociative CANs: the dynamic equilibrium of dissociative bond exchange and the gel point in association with the gel-point temperature of the system [3]. Thus, the gel point temperature of these PU systems may have varied with respect to the BMI introduced and can also be a contributing factor effecting their reprocessing ability.

PU material containing HS, PU-HS20-FO20-PPOBMI-DP6, was deemed reprocessable as it exhibited consistent mechanical properties over reprocessing cycles, as well superior results when compared to original samples exposed to a 120 °C thermal treatment and control sample results (PU-HS20-FO20). It would be of interest to determine how the gel point temperature varied by varying the HS content, determining if indeed the length and structure of the BMI effects the gel point temperature of these systems.

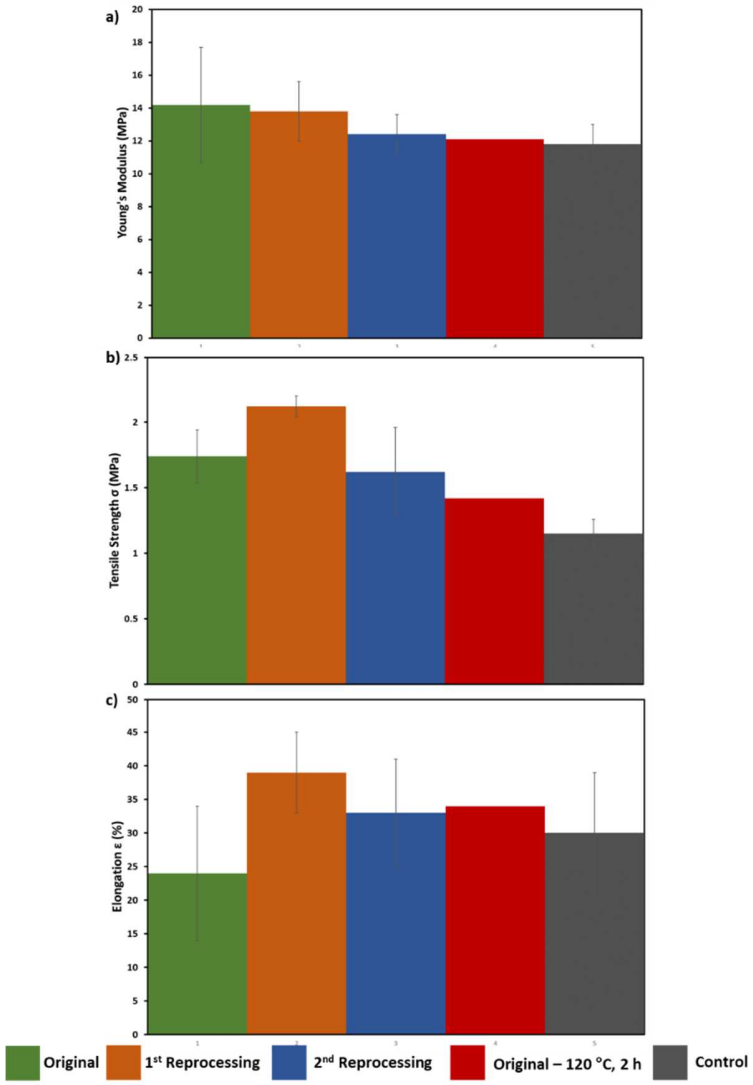

Figure 5 – Comparison of mechanical properties of biobased PU-HS20-FO20-PPOBMI-DP6: original, reprocessed, original heated to 120 °C, and control, (a) Young's modulus, (b) tensile strength (σ), and (c) elongation (ε).

Heat induced self-healing experiments were conducted on dumbbells of synthesized PU materials by the method detailed in the Experimental section. In contrast to previous reported results [30], the heat induced self-healing ability of PU materials synthesized in this study seem to be considerably affected by the BMI length and structure. Detailed results of the self-healing ability of simple PU networks (without HS) is summarized in Table S3.

For the series of PUs containing increasing amount of FO cross-linked by MPBMI, sample PU-FO10-MPBMI would yield the most prevalent recovery of the original material properties. As depicted in Figure 7-a, the sample PU-FO10-MPBMI appears to heal relatively well to the naked eye. Nevertheless, uniaxial tensile test reveal healing of the sample with recovery of 64% of the average original Young's modulus, 41 and 47% of tensile strength and elongation, respectively (Figure 7-b). For the series of PUs with 20% substitution of FO and cross-linked with different BMIs, materials seem to heal relatively similarly with an average recovery of mechanical properties as follows: 39% of Young's modulus, 31% of tensile strength and 50 % elongation. Similarly to sample PU-FO10-MPBMI, sample PU-FO20-MPBMI seems to heal relatively well to the naked eye (Figure-7-c), but as illustrated in Figure 7-d, PU-FO20-MPBMI heals poorly with a recovery of original material properties as follows: 33% Young's modulus, 36% of tensile strength and 58% of elongation. Although, PU-FO20-MPBMI exhibits the highest recovery

in tensile strength with comparison to the other PU of this series, it is still a result considerably diminished when compared to that of reported healing results of a previous study [30]. Thus, although PU-FO10-MPBMI and PU-FO20-MPBMI demonstrate the most prevalent healing results with the shorter aliphatic BMI, the aromatic structure of this BMI impedes its healing ability.

For sample PU-HS20-FO20-PPOBMI-DP6, the stiffness of the dumbbell did not allow for adhesion of the cut ends without an applied pressure. Given that the surface area of the dumbbells, an adhesion test between an overlap of two pieces consisting of 1.5 cm^2 surface area (Figure 7-e) was deemed appropriate. The two pieces of overlapped sample PU-HS20-FO20-PPOBMI-DP6 were exposed to 120 °C for 1h with a 100 g weight to apply slight pressure to the overlap. The overlap sample was then exposed to 60 °C for 48 h. As seen Figure 7-e, the adhesion test displayed good overlap adhesion and the overlap could be submitted to 250 g weight which represented a shear stress of approximately 1.67 x 10^4 Pa (250 g x 10 N / 1000 g)/(1.5 cm^2)). The thermal treatment endured by the overlap allows for a network to be formed by chemical association of the interfacial Diels-Alder moieties. This is a highly favorable result for adhesive applications of such PU systems.

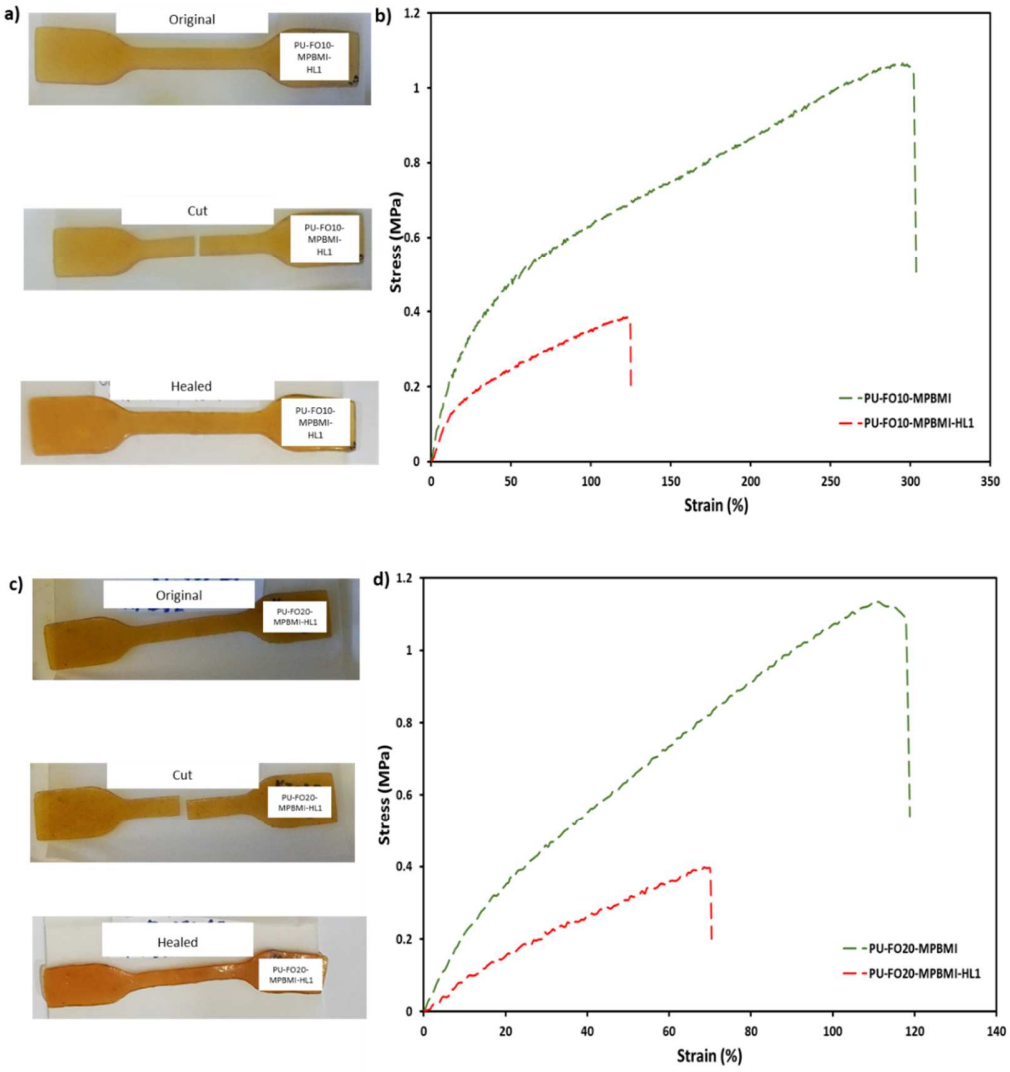

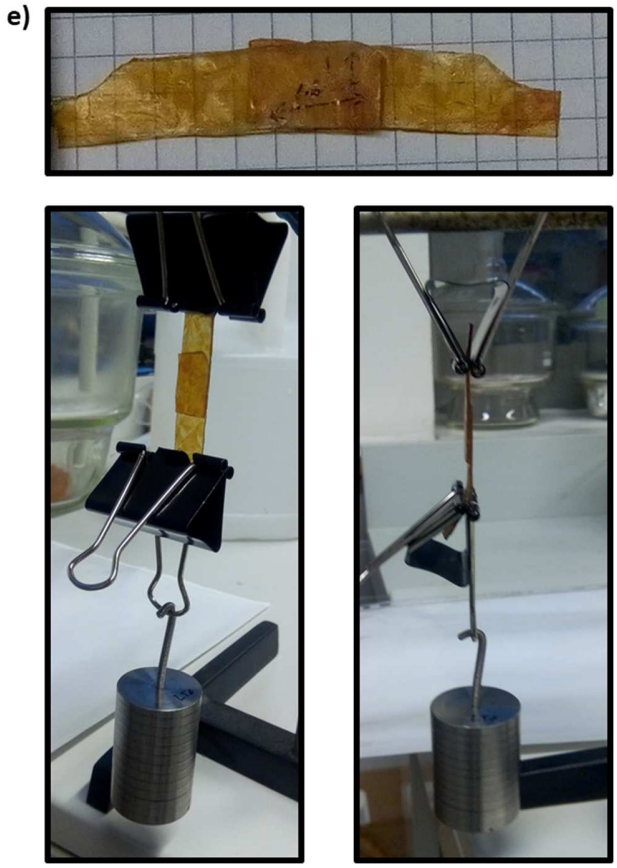

Figure 6 – Observation of healing of materials (a) photographs of original, cut and healed dumbbell sample PU-FO10-MPBMI, (b) stress-strain curves of PU-FO10-MPBMI original and healed sample, (c) photographs of original, cut and healed dumbbell sample PU-FO20-MPBMI, (d) stress-strain curves of PU-FO20-MPBMI original and healed sample, and (e) photographs of adhesion of PU-HS20-FO20-PPOBMI-DP6 films submitted to 250 g load.

Conclusion

A large biobased PU material series based on different cross-linked architectures was successfully elaborated by prioritizing principles for a green chemistry. This study has more particularly examined the effect of various BMIs which varied in length (molar mass) and structure (aliphatic or aromatic) on cross-linked biobased PU network properties such as thermal recyclability and heat induced healing. A PU material series containing varying amounts of FO substitution (10, 20 or 30%) cross-linked by MPBMI exhibited modular mechanical properties largely superior to previous published results [30]. Nevertheless, the rigidity MPBMI diminished the thermal recyclability and heat induced healing ability of the corresponding PU materials compared to previous results [30]. However, the PU material series with 20% substitution of FO and cross-linked by the different BMIs showed that cross-linking by aromatic MPBMI would yield superior mechanical properties compared to the different aliphatic counterparts. The distinguishment of PU networks cross-linked by different BMIs was clearly evidenced. The different cross-linked materials presented superior mechanical properties (when compared to linear reference counterpart) with good thermal recyclability and self-healing behavior. Lastly, the introduction of phase segregation with HS in PU materials was examined. A control and cross-linked architecture was examined. Both architectures would yield superior mechanical properties than all previously synthesized systems. The cross-linked material with HS presented good thermal recyclability and adhesion properties. The corresponding results on these latter systems containing HS provides advanced results to be applied to industrial applications such as adhesives and coatings, for example but not solely for building-based materials.

Developing these PU-based materials provides a thrilling prospect to the notion of reconceiving sustainable material design by elaborating polymer architectures with advanced performances allowing for intrinsic recyclability and a

controlled end of life. Finally, this work constitutes a springboard in the development of innovative, biobased and dynamic macromolecular architectures for a large range of advanced domains by circular and sustainable approaches. These domains include the furniture and interiors, construction, electronics and appliances, automotive, footwear and packaging.

Acknowledgements

The authors would like to thank BPI-France for the funding of Trans'Alg Project and the corresponding consortium. Iterg (France) for kindly providing technical grade oleic acid. The authors would like to thank the R&D Team of Soprema (France). In memory to Pr. Jean-Pierre Pascault (1943-2020), an incredible researcher and a great man who has always sympathetically followed this project.

Keywords: Renewable Resources • Oleic acid • Biobased polymers • Polyurethane • Diels-Alder-Cycloaddition • Reversible network

References

[1] American Chemistry Council, U.S. Resin Production and Sales, 2017. https://plastics.americanchemistry.com/PlasticsStatistics/ACC-PIPS-Year-End-2017-Resin-Stats-vs-2016.pdf. (Accessed 19/11/2019).
[2] D.J. Fortman, J.P. Brutman, G.X. De Hoe, R.L. Snyder, W.R. Dichtel, M.A. Hillmyer, Approaches to Sustainable and Continually Recyclable Cross-Linked Polymers, Acs Sustainable Chemistry & Engineering 6(9) (2018) 11145-11159.
[3] G.M. Scheutz, J.J. Lessard, M.B. Sims, B.S. Sumerlin, Adaptable Crosslinks in Polymeric Materials: Resolving the Intersection of Thermoplastics and Thermosets, Journal of the American Chemical Society 141(41) (2019) 16181-16196.
[4] W. Denissen, J.M. Winne, F.E. Du Prez, Vitrimers: permanent organic networks with glass-like fluidity, Chemical Science 7(1) (2016) 30-38.
[5] C.J. Kloxin, T.F. Scott, B.J. Adzima, C.N. Bowman, Covalent Adaptable Networks (CANs): A Unique Paradigm in Cross-Linked Polymers, Macromolecules 43(6) (2010) 2643-2653.
[6] D. Montarnal, M. Capelot, F. Tournilhac, L. Leibler, Silica-Like Malleable Materials from Permanent Organic Networks, Science 334(6058) (2011) 965-968.
[7] S. Dhers, G. Vantomme, L. Avérous, A fully bio-based polyimine vitrimer derived from fructose, Green Chemistry 21(7) (2019) 1596-1601.
[8] X. Chen, M.A. Dam, K. Ono, A. Mal, H. Shen, S.R. Nutt, K. Sheran, F. Wudl, A Thermally Re-mendable Cross-Linked Polymeric Material, Science 295(5560) (2002) 1698-1702.
[9] H. Ying, Y. Zhang, J. Cheng, Dynamic urea bond for the design of reversible and self-healing polymers, Nature Communications 5 (2014) 3218.
[10] M.M. Obadia, A. Jourdain, P. Cassagnau, D. Montarnal, E. Drockenmuller, Tuning the Viscosity Profile of Ionic Vitrimers Incorporating 1,2,3-Triazolium Cross-Links, Advanced Functional Materials 27(45) (2017) 1703258.
[11] S.A. Canary, M.P. Stevens, Thermally reversible crosslinking of polystyrene via the furan–maleimide Diels–Alder reaction, Journal of Polymer Science Part A: Polymer Chemistry 30(8) (1992) 1755-1760.
[12] C. Carré, Y. Ecochard, S. Caillol, L. Averous, From the synthesis of biobased cyclic carbonate to polyhydroxyurethanes: a promising route towards renewable non-isocyanate polyurethanes, ChemSusChem 12 (2019) 3410.
[13] G. Rivero, L.-T.T. Nguyen, X.K.D. Hillewaere, F.E. Du Prez, One-Pot Thermo-Remendable Shape Memory Polyurethanes, Macromolecules 47(6) (2014) 2010-2018.
[14] T.T. Truong, H.T. Nguyen, M.N. Phan, L.-T.T. Nguyen, Study of Diels–Alder reactions between furan and maleimide model compounds and the preparation of a healable thermo-reversible polyurethane, Journal of Polymer Science Part A: Polymer Chemistry 56(16) (2018) 1806-1814.
[15] E. Dolci, V. Froidevaux, G. Michaud, F. Simon, R. Auvergne, S. Fouquay, S. Caillol, Thermoresponsive crosslinked isocyanate-free polyurethanes by Diels-Alder polymerization, Journal of Applied Polymer Science 134(5) (2017) 44408.
[16] G. Lligadas, Renewable Polyols for Polyurethane Synthesis via Thiol-ene/yne Couplings of Plant Oils, Macromolecular Chemistry and Physics 214(4) (2013) 415-422.
[17] M. Desroches, M. Escouvois, R. Auvergne, S. Caillol, B. Boutevin, From Vegetable Oils to Polyurethanes: Synthetic Routes to Polyols and Main Industrial Products, Polymer Reviews 52(1) (2012) 38-79.
[18] D.V. Palaskar, A. Boyer, E. Cloutet, J.-F. Le Meins, B. Gadenne, C. Alfos, C. Farcet, H. Cramail, Original diols from sunflower and ricin oils: Synthesis, characterization, and use as polyurethane building blocks, Journal of Polymer Science Part A: Polymer Chemistry 50(9) (2012) 1766-1782.
[19] A. Duval, H. Lange, M. Lawoko, C. Crestini, Reversible crosslinking of lignin via the furan-maleimide Diels-Alder reaction, Green Chemistry 17(11) (2015) 4991-5000.
[20] P. Buono, A. Duval, L. Averous, Y. Habibi, Thermally healable and remendable lignin-based materials through Diels – Alder click polymerization, Polymer 133 (2017) 78-88.
[21] A. Duval, G. Couture, S. Caillol, L. Averous, Biobased and Aromatic Reversible Thermoset Networks from Condensed Tannins via the Diels-Alder Reaction, ACS Sustainable Chemistry & Engineering 5(1) (2017) 1199-1207.
[22] C. García-Astrain, L. Avérous, Synthesis and evaluation of functional alginate hydrogels based on click chemistry for drug delivery applications, Carbohydrate Polymers 190 (2018) 271-280.

[23] C. García-Astrain, L. Avérous, Synthesis and behavior of click cross-linked alginate hydrogels: Effect of cross-linker length and functionality, International Journal of Biological Macromolecules 137 (2019) 612-619.
[24] O. Guaresti, C. García–Astrain, R.H. Aguirresarobe, A. Eceiza, N. Gabilondo, Synthesis of stimuli–responsive chitosan–based hydrogels by Diels–Alder cross–linking `click´ reaction as potential carriers for drug administration, Carbohydrate Polymers 183 (2018) 278-286.
[25] K. González, C. García-Astrain, A. Santamaria-Echart, L. Ugarte, L. Avérous, A. Eceiza, N. Gabilondo, Starch/graphene hydrogels via click chemistry with relevant electrical and antibacterial properties, Carbohydrate Polymers 202 (2018) 372-381.
[26] N. Yoshie, S. Yoshida, K. Matsuoka, Self-healing of biobased furan polymers: Recovery of high mechanical strength by mild heating, Polymer Degradation and Stability 161 (2019) 13-18.
[27] Z. Feng, J. Hu, B. Yu, H. Tian, H. Zuo, N. Ning, M. Tian, L. Zhang, Environmentally Friendly Method To Prepare Thermo-Reversible, Self-Healable Biobased Elastomers by One-Step Melt Processing, ACS Applied Polymer Materials 1(2) (2019) 169-177.
[28] A. Gandini, A.J.F. Carvalho, E. Trovatti, R.K. Kramer, T.M. Lacerda, Macromolecular materials based on the application of the Diels–Alder reaction to natural polymers and plant oils, European Journal of Lipid Science and Technology 120(1) (2018) 1700091.
[29] S. Hu, X. Chen, J.M. Torkelson, Biobased Reprocessable Polyhydroxyurethane Networks: Full Recovery of Crosslink Density with Three Concurrent Dynamic Chemistries, ACS Sustainable Chemistry & Engineering 7(11) (2019) 10025-10034.
[30] K.-K. Tremblay-Parrado, L. Avérous, Renewable Responsive Systems Based on Original Click and Polyurethane Cross-Linked Architectures with Advanced Properties, ChemSusChem (2019).
[31] A. Sengupta, T. Dey, M. Ghosh, J. Ghosh, S. Ghosh, Enzymatic Synthesis of Furfuryl Alcohol Ester with Oleic Acid by Candida antarctica Lipase B and Its Kinetic Study, Journal of The Insitution of Engineers (India) 93(1) (2012) 31-36.
[32] V. Froidevaux, M. Borne, E. Laborbe, R. Auvergne, A. Gandini, B. Boutevin, Study of the Diels–Alder and retro-Diels–Alder reaction between furan derivatives and maleimide for the creation of new materials, RSC Advances 5(47) (2015) 37742-37754.
[33] C. Bueno-Ferrer, E. Hablot, M.d.C. Garrigós, S. Bocchini, L. Averous, A. Jiménez, Relationship between morphology, properties and degradation parameters of novative biobased thermoplastic polyurethanes obtained from dimer fatty acids, Polymer Degradation and Stability 97(10) (2012) 1964-1969.
[34] A. Spyros, Quantitative determination of the distribution of free hydroxylic and carboxylic groups in unsaturated polyester and alkyd resins by 31P-NMR spectroscopy, Journal of Applied Polymer Science 83(8) (2002) 1635-1642.

TOC: Further insight on biobased PU architectures cross-liked via the Diels-Alder reaction for the elaboration of biobased covalent adaptable networks (CANs) using the recently developed building block derived from oleic acid, the furan oligomer (FO) and various bismaleimides (BMIs). Biobased PU CANs varied in architecture by the use of BMIs that varied in length and structure as well as altering the PU backbone structure inducing hard segments.

Institute and/or researcher Twitter usernames: @LucAverous

Graphical Abstract